Draft report on predictions of next year atmospheric CO_2

Deliverable 2.5

Authors: Bernardello R., Bopp L., Ilyina T., Li H., Mignot J., and Tourigny E.

This project received funding from the Horizon 2020 programme under the grant agreement No. 821003.

Document Information

GRANT AGREEMENT	821003
PROJECT TITLE	Climate Carbon Interactions in the Current Century
PROJECT ACRONYM	4C
PROJECT START DATE	2019-06-01
RELATED WORK PACKAGE	WP2
RELATED TASK(S)	T2.4
LEAD ORGANIZATION	MPG
AUTHORS	Bernardello R., Bopp L., Ilyina T., Li H., Mignot J., and Tourigny E.
SUBMISSION DATE	2021-03-31
DISSEMINATION LEVEL	PU

History

DATE	SUBMITTED BY	REVIEWED BY	VISION (NOTES)
30/03/2021	Hongmei Li		
31:03/2021		P. Friedlingstein	

Please cite this report as: Bernardello R., Bopp L., Ilyina T., Li H., Mignot J., and Tourigny E. (2021), Draft report on predictions of next year atmospheric CO_2, D2.5 of the 4C project

Table of Contents

List of tables

List of figures

About 4C

Climate-Carbon Interactions in the Coming Century (4C) is an EU-funded H2020 project that addresses the crucial knowledge gap in the climate sensitivity to carbon dioxide emissions, by reducing the uncertainty in our quantitative understanding of carbon-climate interactions and feedbacks. This will be achieved through innovative integration of models and observations, providing new constraints on modelled carbon-climate interactions and climate projections, and supporting Intergovernmental Panel on Climate Change (IPCC) assessments and policy objectives.

Executive Summary

The objective of 4C WP2 is to develop the capability of 3 European ESMs (IPSL-ESM, MPI-ESM, EC-Earth) to predict the near-term evolution of carbon sinks, atmospheric CO_2, and climate in response to future emissions. To predict the atmospheric CO_2, IPSL-ENS, MPG, and BSC are developing/ have developed their emission-driven ESM prediction system enabling prognostic atmospheric CO_2 concentration. This deliverable (1) describes the 4C emission-driven prediction system and how each group initializes the ESM predictions, (2) presents the reconstructions in the past years and predictions into next years on atmospheric CO_2 and the corresponding air-land and air-sea CO_2 fluxes, and (3) shows how much the COVID19 pandemic induced emission reduction affect the global carbon cycle and atmospheric CO_2 concentration.

Keywords

Earth System Models, Atmospheric CO_2, Reconstruction, Near-term Predictions, Carbon cycle

1 Introduction of the prediction systems

To facilitate prediction of the next year atmospheric CO_2, all the three 4C prediction model centers have endeavored to develop their decadal prediction systems based on emission-driven simulations with prognostic atmospheric CO_2 concentration. Given a new dimension of freedom, the climate states and circulations in the emission-driven model requires new adjustments and therefore are different than in the concentration-driven model, a separate spinup and control simulation under the emission-driven framework is necessary.

As the anthropogenic emissions in the last year was drastically reduced due to Covid19 pandemic relative to previous years (Le Quéré et al. 2020; Forster et al. 2020), the CMIP6 baseline scenario (i.e., ssp245) are not suitable anymore for the predictions. For these runs, we use adjusted CO_2 emissions, other greenhouse gas concentrations, aerosol and ozone forcings from a newly endorsed CMIP6 CovidMIP (Jones et al. 2021; Lamboll et al. 2020; Fiedler et al. 2020). In this study, we use the CovidMIP two-year blip scenario forcings for our simulations from year 2015 and for the period before we use the CMIP6 historical forcings. To investigate the influence of the emission reductions, we have also shown the changes of global carbon cycle in comparing with the predictions under ssp245 baseline forcings. If it is not specifically stated, the results shown in this report are driven by CMIP6 historical plus two-year blip scenario forcings.

1.1 IPSL-CM6A-LR

The IPSL Earth System numerical model is composed of three models (atmospheric, oceanic, and terrestrial biosphere) that are coupled together. We refer to this model as IPSL-CM6A-LR. The three models are LMDZ (v6A-LR, Hourdin et al., 2020) for the atmosphere general circulation, NEMO (v3.6, Aumont et al., 2015; Madec et al., 2017; Rousset et al., 2015; Vancoppenolle et al., 2009) for the oceanic general circulation, and ORCHIDEE (v2.0, Peylin et al., 2020, in preparation) for the land surface processes respectively. The NEMO model further encompasses three main components: the ocean physics NEMO-OPA (Madec et al., 2017), the sea ice dynamics and thermodynamics NEMO-LIM3 (Rousset et al., 2015; Vancoppenolle et al., 2009), and the ocean biogeochemistry NEMO-PISCES (Aumont et al., 2015). Overall, this constitutes the reference version of IPSL-CM6A-LR which was used for the CMIP6 experiment (Boucher et al., 2020).

Predictions based on the IPSL-CM6A-LR climate model are initialized from a global century long simulation in which anomalies of global EN4 sea surface temperature and Atlantic sea surface salinity presented by Reverdin et al. (2019) have been nudged into the climate model. The nudging procedure is described by Estella-Perez et al. (2020). It includes in particular a variable nudging strength depending on the upper mixed layer depth, as described in Ortega et al 2016. Furthermore, the low frequency modulation of sea surface salinity anomalies as reconstructed by Reverdin et al (2019) are combined to the climatology of SSS from EN4. There is no assimilation of subsurface ocean, sea ice, biogeochemistry or atmospheric observations.

1.2 MPI-ESM1.2-LR

MPI-ESM1.2-LR refers to low resolution version of MPI-ESM with atmosphere ~200km in the horizontal and 47 vertical levels and ocean ~150km in horizontal and 40 vertical levels (Mauritsen et al., 2019). We nudge atmospheric 3D full-field temperature, vorticity, divergence, and surface pressure from the European Centre for Medium-Range Weather Forecasts (ECMWF) Re-Analysis ERA40 (Uppala et al. 2005) for the period 1958-1979 and ERA5 (Hersbach et al. 2020) for the period from 1980-2020. For the ocean component, we use Ensemble Kalmann Filter (EnKF, refer to Brune et al. 2018) method to assimilate full fields of subsurface profiles of temperature and salinity from EN4 data (Good et al. 2013). The land and ocean biogeochemical component is indirectly initialized via the atmospheric and oceanic data assimilation in the fully coupled ESM.

Due to the unavailability of ocean reanalysis data from ECMWF for the recent years, we had to switch our ocean initialization and implemented EnKF assimilation method. It is computationally more expensive than our previous system based on nudging, and it requires several cycles of spinup run for the ocean circulation to reach an quasi-equilibrium state before the reconstruction run.

1.3 EC-EARTH3-CC

EC-Earth3-CC is the carbon cycle version of the EC-Earth3 Earth System Model. A detailed description of model components can be found in Döscher et al. (2021). Initial conditions for EC-Earth3-CC are obtained from three different procedures for atmosphere, land vegetation and ocean. For the ocean, the procedure includes restoring of SST and SSS as well as 3D temperature and salinity Newtonian dumping below the mixed layer. We use the restoring timescale distribution of Sanchez-Gomez et al. (2016) below the mixed layer which varies between 10 days (up to 800m) and 360 days (below 800m). At the surface SST is restored using a feedback coefficient between flux and temperature of -200 W/m2/K while the feedback parameter for freshwater fluxes is set at -750 mm/day. We leave a 10-times weaker 3D nudging band between 15ºS-15ºN. The reference dataset used for surface restoring is the ECMWF Ocean Reanalysis System 5 (ORAS5) (Zuo et al., 2019), while the 3D nudging is applied towards EN4 (Good et al. 2013). Finally, the atmospheric forcing used is the DRAKKAR forcing set DFS5.2 (Dussin et al. 2016) which is based on the ERA-40 and Era-Interim reanalyses for the period 1958-1979 and ERA5 for the period 1979-2020. Sea Ice, as well as ocean biogeochemistry, are let free to evolve in response to the constrained ocean physics. . The atmospheric initial conditions are obtained from the ERA5 reanalysis from ECMWF, which have been interpolated to the EC-Earth3 Standard Resolution configuration of T255/N128 in the horizontal and 91 vertical levels, using full-pos from openIFS cycle 40r1. For the land vegetation the LPJ-GUESS dynamic vegetation model is forced offline using the ERA-20C reanalysis for the period prior to 1979 and ERA5 from 1979-2020, for consistency with the ocean reanalyses used for generating the Ocean ICs (more details in D2.2).

Because of this procedure EC-Earth3-CC does not have interactive atmospheric carbon for the reconstructions. A full assimilation coupled procedure is under development and it will be tested with EC-Earth3-CC as soon as ready. At the moment, the forecast of atmospheric CO_2 is realized by initializing the atmosphere with uniform CO_2 concentration from the CMIP6 CovidMIP dataset.

Table 1: Overview of 4C emission-driven prediction systems

MODEL	IPSL-CM6A-LR	MPI-ESM1.2-LR	EC-EARTH3-CC
Resolution Atmosphere	2.5°x1.3°, 79 levels	T63, 47 levels	T255, 91 levels
Rosolution Ocean	1°, 75 levels	1.5°, 40 levels	1°, 75 levels
Initialization Atmosphere	None	ERA-40 before 1979 and ERA5 from 1980: Vorticity, divergence, log(p), T; full field with nudging	ERA5 full-field
Initialization Ocean	Nudging towards SST (ERSSTv5) and SSS (doi: 10.6096/SSS-BINS-ATL) using a restoring coefficient dependent on the mixed layer depth (Ortega et al 2017)	EN4 3D full field T and S with ensemble kalmann Filter	EN4 3D nudging T and S with weaker nudging band around equator. SST and SSS restoring to ORAS5. Atmospheric forcing: DFS5.2 1958-1979 + ERA5 1980 – 2020.
Initialization Land		Indirectly initialized by atmospheric and oceanic data assimilation within the fully coupled ESM	LPJ-GUESS forced offline with ERA5 1979-2020 after preindustrial spinup+transient up to 1979.
Ensemble Size	10 members	10 members	10 members
Period of reconstruction	1901-2016	1958-2020	1958-2020

Hindcasts and forecasts	10 years starting from Jan 1st 1961-2016	5 years starting from Nov.1st 1965-2020	5 years starting from Nov.1st 1975-2020 (in progress)
External forcings	CMIP6 historical (1958-2014) plus ssp245 baseline (2015-)	CMIP6 historical (1958-2014) plus ssp245 baseline (2015-) and CovidMIP Two-year blip (2020-) scenario	CMIP6 historical (1958-2014) plus ssp245 baseline (2015-) and CovidMIP Two-year blip (2020-) scenario
References	Boucher et al. (2020)	Mauritsen et al. (2019)	Sanchez-Gomez et al (2016)

2 Historical simulations of the atmospheric CO_2 concentration

Figure 1 shows the prognostic atmospheric CO_2 concentration from EC-Earth3-CC and MPI-ESM1.2-LR emission-driven historical uninitialized simulations in comparison to the CMIP6 prescribed CO_2 concentration and the NOAA-GML data measurements. As the atmospheric CO_2 concentration is acumulative quantity, the deviations in the previous historical years when less data constraints are available show impact on the concentration in recent years. For instance, the models could not capture the plateau of atmospheric carbon increment in the 1940-1950s, this ends up with a ~10ppm higher atmospheric CO_2 concentration than the observations for MPI-ESM1.2-LR and ~30ppm for EC-Earth3-CC. This model bias needs to be corrected in the reconstructions and predictions in order to compare with observations. For EC-Earth3-CC, the deviation of prognostic atmospheric CO_2 concentration relative to the CMIP6 input4MIPs data starts from the 1920s until 1950s with a steeper slope, indicating a larger atmospheric CO_2 increment during this period. However, as shown from the consistent slope of the curves, the increment of atmospheric CO_2 after 1950s is similar to that in the CMIP6 input4MIPs and NOAA-GML observations.

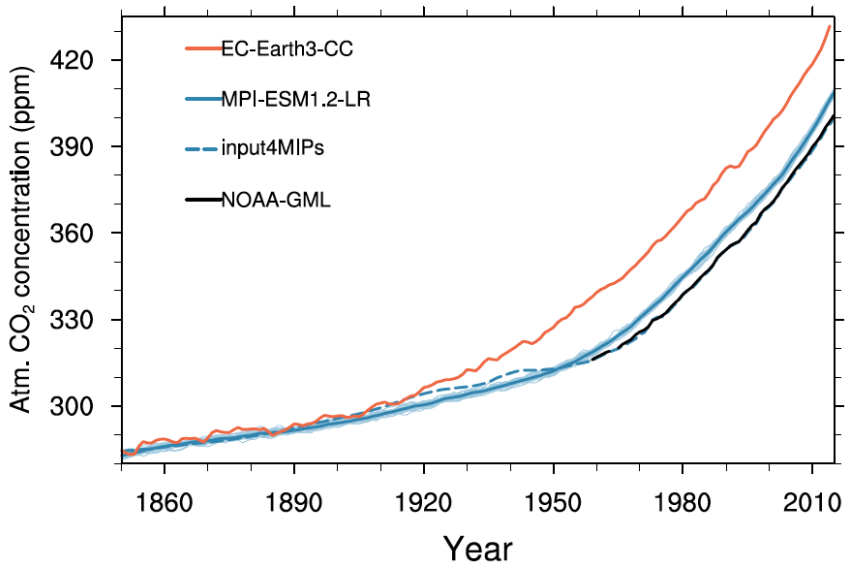

Figure 1. Time series of the atmospheric CO_2 concentration from EC-Earth3-CC and MPI-ESM1.2-LR historical uninitialized simulations in comparison with the CMIP6 prescribed atmospheric CO_2 concentration from input4MIPs and the NOAA-GML observations (Dlugokencky and Tans 2020).

Historical simulations of atmospheric CO_2 with the IPSL-CM6A climate model in its emission-driven mode are still underway. For these emission-driven simulations, two important improvements were brought to the IPSL-CM6A-LR reference version. Previously, in ORCHIDEE, the downregulation was modelled as a logarithmic function of the increase of the CO_2 concentration relative to 380 ppm (following Sellers et al., 1996). However, at high CO_2 concentration values (700 ppm and above) the limiting effect of nitrogen on carbon absorption by the terrestrial biosphere was probably overestimated. A new parametrization of the downregulation has been introduced. It is now modelled as a hyperbolic function of the increase of the CO_2 concentration relative to 380 ppm. Furthermore, in LMDZ, interactive CO_2 and CO_2 transport capabilities were introduced. The coupled model is now forced by emissions as opposed to being forced by CO_2 concentration. Carbon fluxes from the terrestrial biosphere and from the ocean to the atmosphere are taken into account (at 15-minute and 1-day frequency, respectively). The model further computes the atmospheric CO_2 concentration and it models the atmospheric CO_2 transport. This allows for biogeochemical and oceanic processes to react to the spatial distribution of the CO_2 concentration but also for the computation of the radiative effect of the CO_2.

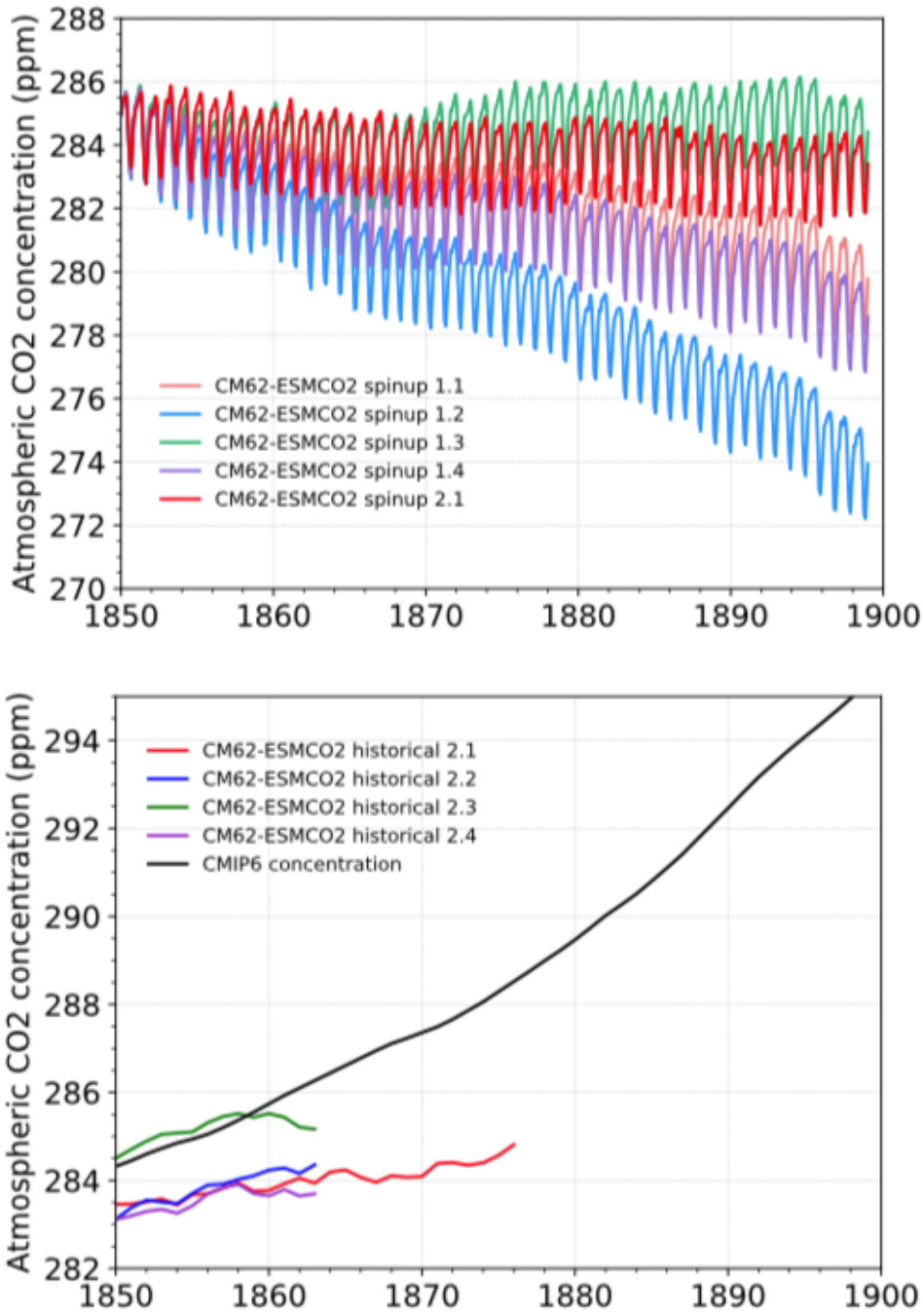

Figure 2 : Spin-up (upper panel) and historical (lower panel - underway) simulations with IPSL-CM6A. See text for details.

Because land and ocean carbon fluxes are slightly drifting as well as not equilibrating towards net zero fluxes in the pre-industrial control simulation, we had to determine appropriate corrections to be applied, so that atmospheric CO_2 is stable in the interactive carbon simulation. Two sets of simulations were performed. These

were performed with the same model where atmospheric transport is enabled, the atmospheric CO_2 concentration is computed, and the radiative code sees the transported atmospheric CO_2. The two sets however differ on whether the carbon fluxes are subject to a constant atmospheric CO_2 concentration (set 1), or not (set 2). Each set is comprised of 4 simulations where no correction was applied (1), correction was applied to the oceanic component only (2), to the land component only (3) or to both (4). We refer to a given simulation by both its set number and its own number (e.g., simulation 1.3 is simulation number 3 of set 1). The results of these simulations are shown in Figure 2 which illustrates that applying a correction to the land component provides the best results. We have run these simulations until reaching a satisfactory equilibrium. Using the Set 2 simulations we have then run historical simulations. These are currently running and no definitive conclusion can be made yet. The retained simulation will be the one providing the best global CO_2 growth rate and inter hemispheric gradient.

3 Reconstruction and prediction of the atmospheric CO_2 concentration and CO_2 fluxes

3.1 Reconstruction

By assimilating atmospheric and oceanic observational data products into EC-Earth3-CC and MPI-ESM1.2-LR decadal prediction system, we can reproduce the variations of the historical global carbon cycle globally. As shown in Figure 3, the atmospheric carbon growth, net carbon flux into the ocean and net carbon flux into the land reconstructed by MPI-ESM1.2-LR show consistent variations with the global carbon budget (GCB2020, Friedlingstein et al., 2020) in the last decades with high correlations of 0.82, 0.97, and 0.73, respectively. As EC-Earth3-CC land and ocean components are reconstructed separately based on stand-alone models; therefore, no prognostic atmospheric CO_2 is available from the reconstruction. The net carbon flux into the ocean and the net carbon flux into the land reconstructed by EC-Earth3-CC show coherent variations as GCB2020 with correlations of 0.89 and 0.68, respectively.

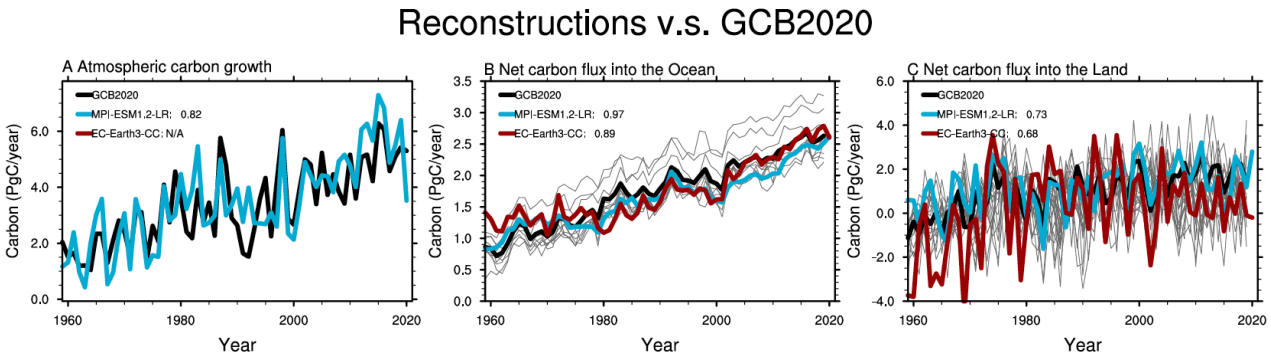

Figure 3. Time series of (A) atmospheric carbon growth rate, (B) carbon fluxes into the ocean, and (C) carbon fluxes into the land from EC-Earth3-CC and MPI-ESM1.2-LR reconstructions in comparison with Global Carbon Budget (GCB 2020, Friedlingstein et al., 2020). The thin blue curves in B and C show individual GCB stand-alone model results. The numbers in the legend show the correlation coefficients between reconstructions and GCB2020. Note that the EC-Earth3-CC land and ocean components are reconstructed separately, therefore no prognostic atmospheric CO_2 is available from the reconstruction.

3.2 Hindcast skill

Retrospective predictions based on MPI-ESM1.2-LR emission-driven hindcasts, which are initiated from the reconstructions, show predictive skill in the atmospheric carbon growth rate, air-sea CO_2 fluxes, and air-land CO_2 fluxes (Figure 4). The air-sea CO_2 fluxes have higher predictive skill up to 5 years, and the detrended air-land CO_2 fluxes and atmospheric carbon growth rate show predictive skill of 2 years.

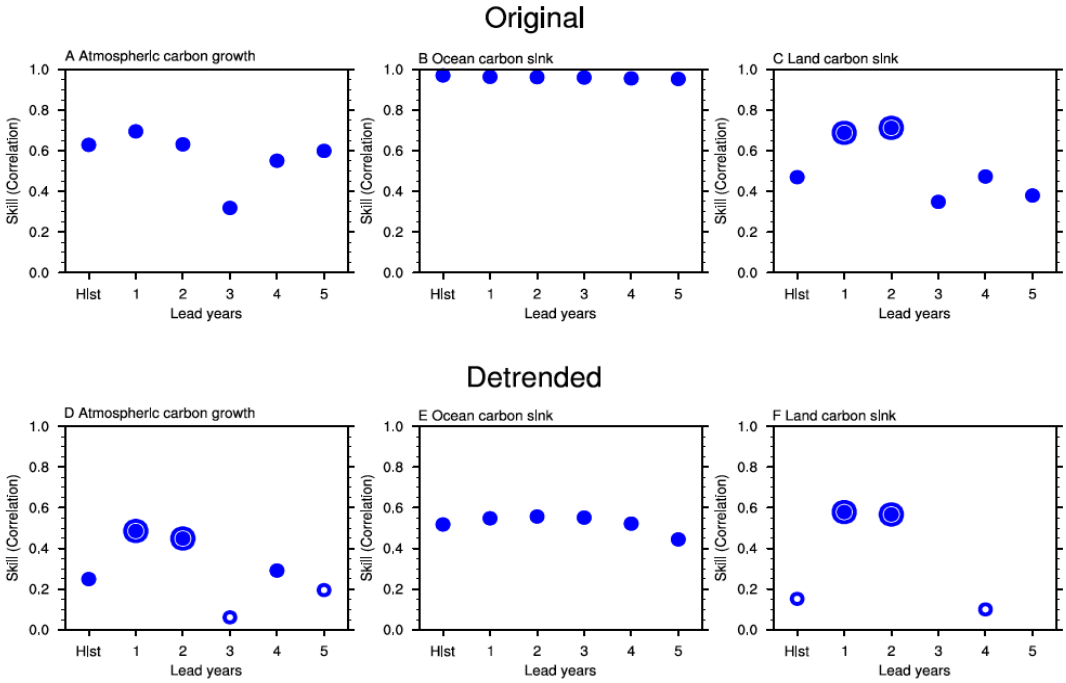

Figure 4. Predictive skill of atmospheric carbon growth rate (A and D), air-sea CO_2 (B and E) and air-land CO_2 fluxes (C and F) from MPI-ESM1.2-LR reference to Global Carbon Budget (GCB 2020, Friedlingstein et al., 2020)). A-C show results of anomaly correlation coefficients from original time series, and D-F show results from detrended time series. All are based on annual mean time series for the time period from 1970-2019. The filled circles show significant predictive skill at 95% confidence level and the additional larger circles indicate improved significant predictive skill due to initialization in comparing to the freely historical simulations. We use a nonparametric bootstrap approach (Goddard et al., 2013) to assess the significance of predictive skill.

3.3 Predictions into next years

Figure 5 shows the hindcasts together with predictions of atmospheric CO_2 concentration and increment. The model simulations show deviations relative to the NOAA-GML observations of atmospheric CO_2 concentration (Figure 5A). We applied bias correction (i.e., mean state and trend from 2010-2020) to model predictions and end up with a very close evolution of the atmospheric CO_2 concentration towards observation (Figure 5B). The coherence of the evolution is shown at all the lead time, the decrease of skill in capturing interannual variations along with lead time is more obvious in the atmospheric CO_2 increment rather than the concentration itself (Figure. 5D).

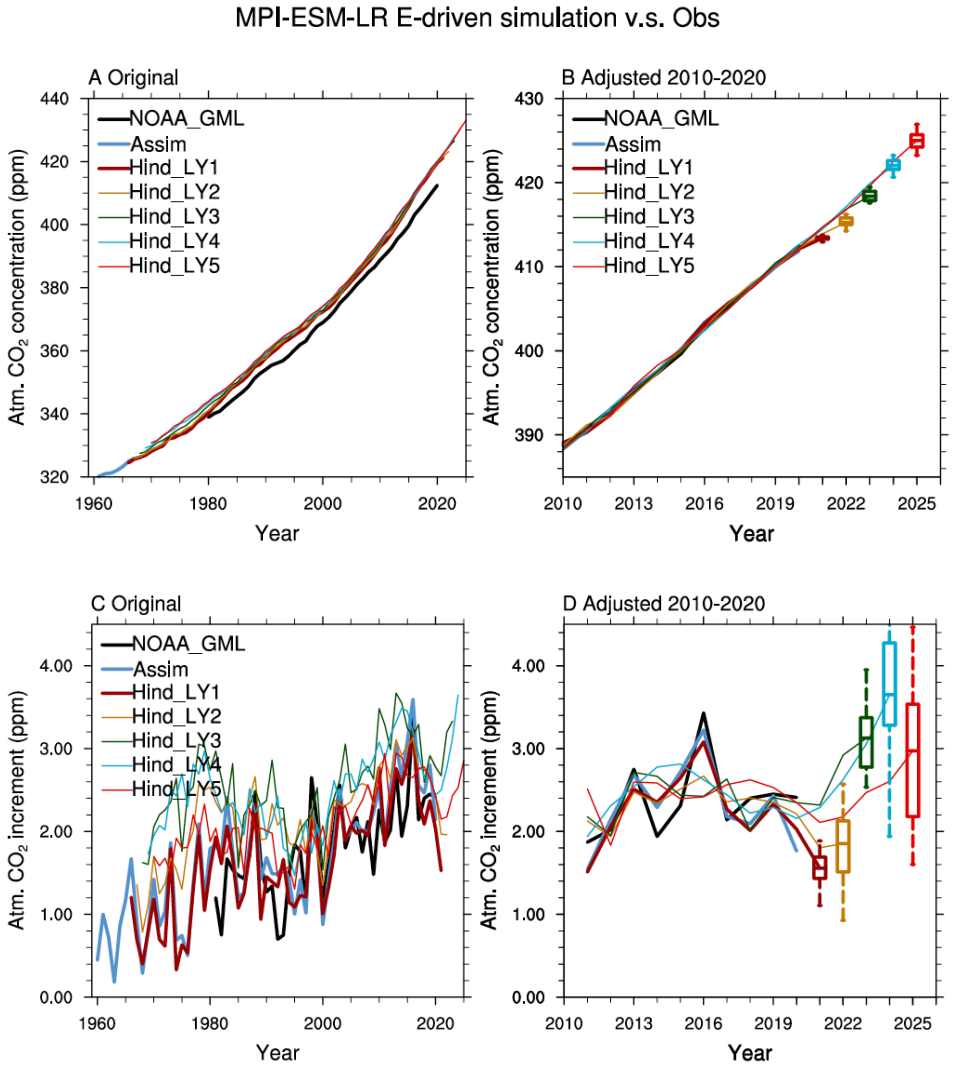

Figure 5. Reconstruction and predictions of the atmospheric CO_2 concentration (A-B) and increment (C-D) from MPI-ESM1.2-LR simulations. A and C are original model outputs, B and D the time series are adjusted towards observation regarding to the mean and trend of atmospheric CO_2 concentration from 2010-2020. The color box-plots in B and D show the predictions starting from 2020 at lead time from 1 to 5 years. The NOAA_GML data are from Dlugokencky and Tans (2020).

Figure 6 shows the first attempt at forecasting future atmospheric CO_2 concentration with EC-Earth3-CC. Although the model predicts a clear difference between the ssp245-baseline and the COVID 2-yr blip scenarios in atmospheric CO_2, this is mainly due to the different initial CO_2 concentration and emissions rather than to a

difference in the behavior of the land and ocean C sinks which is almost identical between the two scenarios. To note the rather limited spread in the two ensembles during the first forecast year, which may be due to our choices of perturbing only the atmosphere and of initializing the predictions with a uniform atmospheric CO_2 field. A solution for both aspects is under development and it will be ready for next year predictions and the hindcasts.

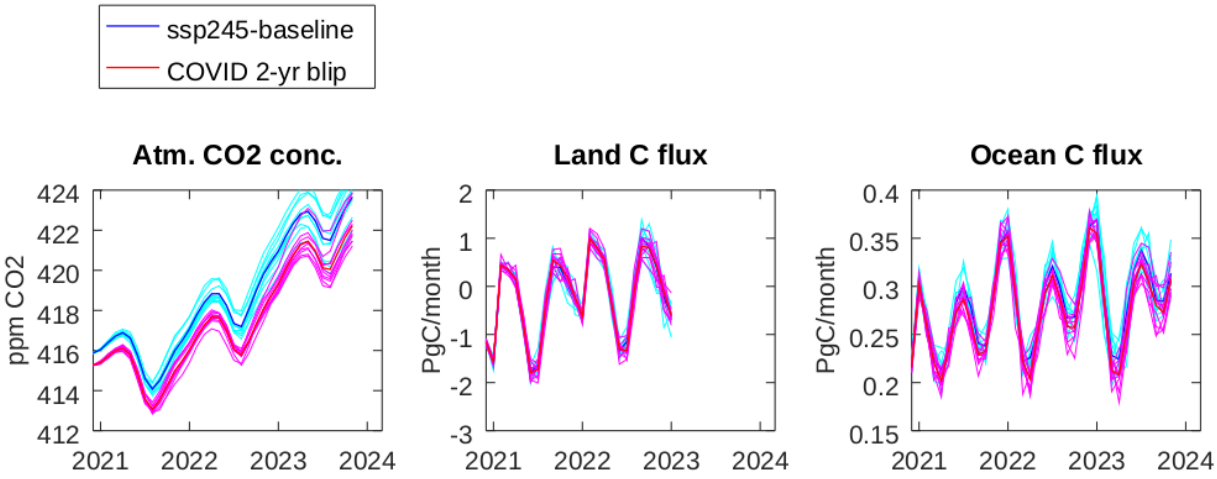

Figure 6. EC-Earth3-CC forecast for the period 1st Nov 2020 to 31st Oct 2023 of atmospheric CO_2 concentration, land and ocean C sink. Plots show monthly values. Cyan/magenta thin lines represent the single members of the respective ensembles: ssp245/COVID 2-yr blip, while the thick blue/red lines represent the respective ensemble means. The land C flux prediction reaches only the end of 2022 because LPJ-GUESS is designed to output only at the end of the year.

Prediction of atmospheric CO_2 concentration and increment from EC-Earth3-CC and MPI-ESM1.2-LR (Figure 7) show increase of atmospheric CO_2 concentration in general but with a lower rate in the next years than normal years because of the emission reductions. The increase of atmospheric CO_2 concentration in 2021 is predicted to be 0.80±0.31 ppm and 1.56±0.23 ppm by EC-Earth3-CC and MPI-ESM1.2-LR, respectively. The values are smaller than those for normal year atmospheric CO_2 increment of about 2.5 ppm (refer to Friedlingstein et al., 2020). As the emissions recover to baseline in 2 years following the CovidMIP two-year blip scenario, the atmospheric increment in year 2022 will be higher than in 2021 with 3.25±0.51ppm and 1.80±0.28ppm from EC-Earth3-CC and MPI-ESM1.2-LR predictions, respectively, and it turns to be higher than 2.5ppm for the next years from 2023-2025 in MPI-ESM1.2-LR predictions. With regards to the predictive skill, as shown in Figure 4, the predictions in lead time up to 2 years have higher confidence than the predictions towards longer lead time of 3-5 years.

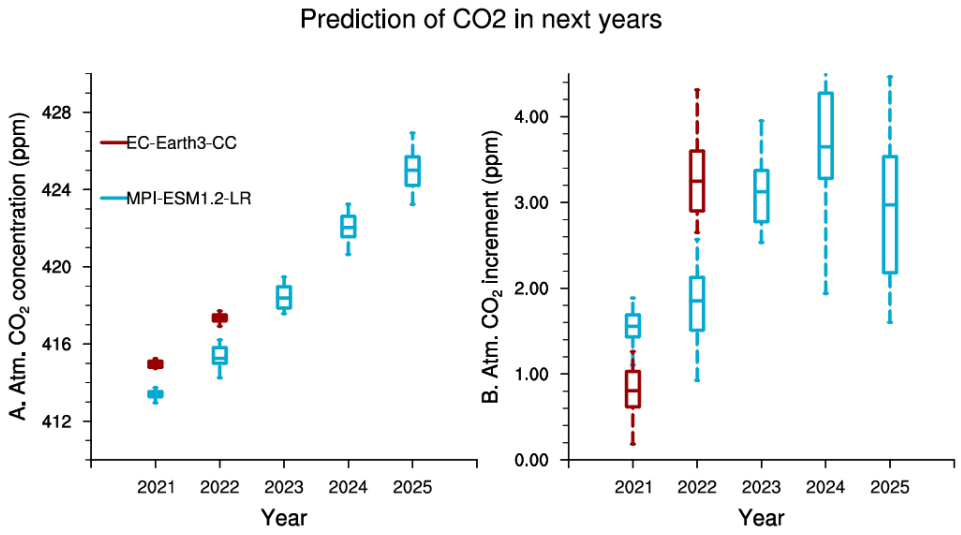

Figure 7. Predictions of atmospheric CO_2 concentration (left) and increment (right) in the next years from EC-Earth3-CC and MPI-ESM1.2-LR simulations. The boxes show the mean and spread distribution from 10 ensemble members. The atmospheric CO_2 increment from EC-Earth3-CC is calculated from CO_2 concentration in December, i.e., Dec. 2021 minus Dec. 2020 and Dec. 2022 minus Dec. 2021 for year 2021 and 2022, respectively. The atmospheric CO_2 concentration from MPI-ESM1.2-LR is bias corrected as in Figure 5 and the increment is based on annual mean data.

4 Influence of the emission reductions due to COVID-19 on the global carbon cycle

To quantify the influence of emission reductions due to COVID-19 on the atmospheric CO_2 concentration and CO_2 fluxes, we calculate the difference between the simulations under two-year blip forcings and those under esm-ssp245 baseline forcings (Figure 8). EC-Earth3-CC and MPI-ESM1.2-LR are quite consistent in the atmospheric CO_2 concentration changes. Discrepancies are shown in the CO_2 fluxes especially for the spread of ensemble members, the internal variability seems larger in MPI-ESM1.2-LR than in EC-Earth3-CC.

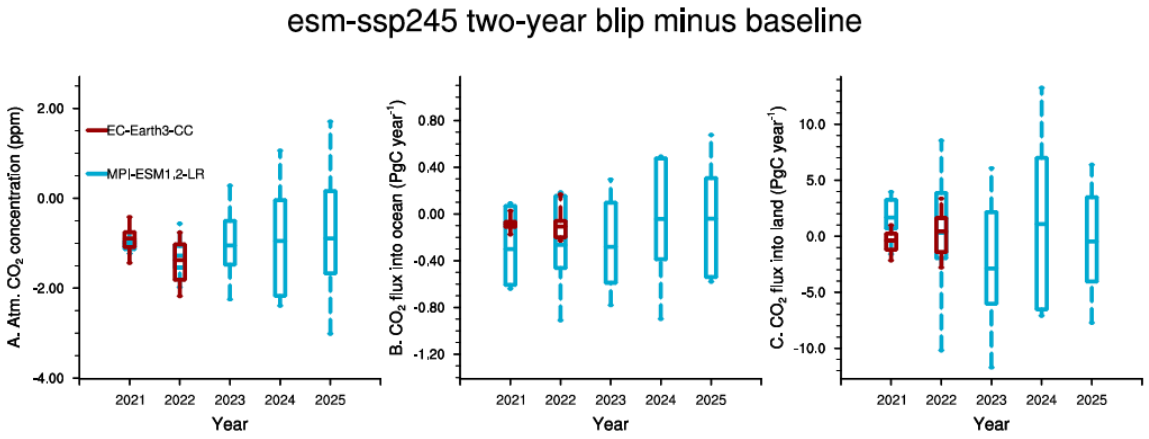

Figure 8. Changes in atmospheric CO_2 concentration (A), CO_2 flux into the ocean (B), and CO_2 flux into the land (C) due to COVID-19 induced emission reductions. Shown are the differences for EC-Earth3-CC and MPI-ESM1.2-LR predictions using CovidMIP two-year blip and ssp245 baseline forcings.

5 Conclusions

The emission-driven simulations enable prognostic atmospheric CO_2. With 4C prediction systems based on ESMs with interactive carbon cycle driven by CO_2 emissions, we present our first results of predictions in atmospheric CO_2 in the next years, the increment of atmospheric CO_2 is predicted to be smaller relative to normal years due to the drastic COVID-19 pandemic induced emission reductions.

MPI-ESM1.2-LR reconstruction and hindcasts show the ability of ESMs based decadal prediction system in capture and predict the variations of atmospheric carbon growth rate and the CO_2 fluxes. The first 2 year predictions show significant predictive skill even in the multi-year variations with detrended time series.

6 Publications

Li, H., T. Ilyina, A. Spring, R. Bernardello, L. Bopp, J. Mignot, E. Tourigny, and other coauthors (2021), Predictions of atmospheric CO_2 and global carbon cycle, BAMS, in preparation.

7 References

Brune, S., Düsterhus, A., Pohlmann, H., Müller, W., & Baehr, J. (2018). Time dependency of the prediction skill for the North Atlantic subpolar gyre in initialized decadal hindcasts. Climate Dynamics, 51(5–6), 1947–1970.

Dlugokencky, E., & Tans, P. (2020). Trends in atmospheric carbon dioxide. National Oceanic and Atmospheric Administration, Earth System Research Laboratory (NOAA/ESRL). Retrieved from http://www.esrl.noaa.gov/gmd/ccgg/rends/global.html

Döscher, R., Acosta, M., Alessandri, A., Anthoni, P., Arneth, A., Arsouze, T., Bergmann, T., Bernardello, R., Bousetta, S., Caron, L.-P., Carver, G., Castrillo, M., Catalano, F., Cvijanovic, I., Davini, P., Dekker, E., Doblas-Reyes, F. J., Docquier, D., Echevarria, P., Fladrich, U., Fuentes-Franco, R., Gröger, M., v. Hardenberg, J., Hieronymus, J., Karami, M. P., Keskinen, J.-P., Koenigk, T., Makkonen, R., Massonnet, F., Ménégoz, M., Miller, P. A., Moreno-Chamarro, E., Nieradzik, L., van Noije, T., Nolan, P., O'Donnell, D., Ollinaho, P., van den Oord, G., Ortega, P., Prims, O. T., Ramos, A., Reerink, T., Rousset, C., Ruprich-Robert, Y., Le Sager, P., Schmith, T., Schrödner, R., Serva, F., Sicardi, V., Sloth Madsen, M., Smith, B., Tian, T., Tourigny, E., Uotila, P., Vancoppenolle, M., Wang, S., Wårlind, D., Willén, U., Wyser, K., Yang, S., Yepes-Arbós, X., and Zhang, Q.: The EC-Earth3 Earth System Model for the Climate Model Intercomparison Project 6, Geosci. Model Dev. Discuss. [preprint], https://doi.org/10.5194/gmd-2020-446, in review, 2021.

Dussin, R., B. Barnier and L. Brodeau (2016), Up-dated description of the DFS5 forcing data set: The making of Drakkar forcing set DFS5. DRAKKAR/MyOcean Report 01-04-16, LGGE, Grenoble, France.

Fiedler, S., K. Wyser, J. Rogelj, and T. van Noije, 2020: Radiative effects of reduced aerosol emissions during the COVID-19 pandemic and the future recovery, Earth's Future, submitted. https://www.essoar.org/doi/10.1002/essoar.10504704.1

Friedlingstein, P., O'Sullivan, M., Jones, M. W., Andrew, R. M., Hauck, J., Olsen, A., . . . others (2020). Global carbon budget 2020. Earth System Science Data, 12 (4), 3269-3340.

Forster, P. M. et al. (2020), Current and future global climate impacts resulting from COVID-19. Nature Climate Change, doi: 10.1038/s41558-020-0883-0.

Goddard, L., Kumar, A., Solomon, A., Smith, D., Boer, G., Gonzalez, P., . . . others (2013). A vericationframework for interannual-to-decadal predictions experiments. Climate Dynamics, 40 (1-2), 245-272.

Good, S. A., Martin, M. J., & Rayner, N. A. (2013). EN4: Quality controlled ocean temperature and salinity profiles and monthly objective analyses with uncertainty estimates. Journal of Geophysical Research: Oceans, 118, 6704–6716. https://doi.org/10.1002/2013JC009067

Hersbach, H., Bell, B., Berrisford, P., Hirahara, S., Horányi, A., Muñoz-Sabater, J., ... & Thépaut, J. N. (2020). The ERA5 global reanalysis. Quarterly Journal of the Royal Meteorological Society, 146(730), 1999-2049.

Jones, C.D., et al. (2021) The climate response to emissions reductions due to COVID-19: Initial results from CovidMIP. Geophys. Res. Letters, https://doi.org/10.1029/2020GL091883

Lamboll, R. D., Jones, C. D., Skeie, R. B., Fiedler, S., Samset, B. H., Gillett, N. P., Rogelj, J., and Forster, P. M. (2020): Modifying emission scenario projections to account for the effects of COVID-19: protocol for Covid-MIP, Geosci. Model Dev. Discuss. https://doi.org/10.5194/gmd-2020-373, in review.

Le Quéré, C., R.B. Jackson, M.W. Jones, A.J.P. Smith, S. Abernethy, R.M. Andrew, A.J. De-Gol, D.R. Willis, Y. Shan, J.G. Canadell, P. Friedlingstein, F Creutzig, G.P. Peters (2020). Temporary reduction in daily global CO_2 emissions during the COVID-19 forced confinement. Nature Climate Change. https://doi.org/10.1038/s41558-020-0797-x

Mauritsen, T., Bader, J., Becker, T., Behrens, J., Bittner, M., Brokopf, R., ... & Roeckner, E. (2019). Developments in the MPI-M Earth System Model version 1.2 (MPI-ESM1. 2) and its response to increasing CO_2. Journal of Advances in Modeling Earth Systems, 11(4), 998-1038.

Ortega, P., Guilyardi, E., Swingedouw, D. et al. Reconstructing extreme AMOC events through nudging of the ocean surface: a perfect model approach. Clim Dyn 49, 3425–3441 (2017). https://doi.org/10.1007/s00382-017-3521-4 Peters, G. P. et al. (2017), Towards real-time verification of CO_2 emissions. Nat. Clim. Change 7, 848-850

Uppala, S. M., Kållberg, P. W., Simmons, A. J., Andrae, U., Bechtold, V. D. C., Fiorino, M., ... & Woollen, J. (2005). The ERA-40 re-analysis. Quarterly Journal of the Royal Meteorological Society: A journal of the atmospheric sciences, applied meteorology and physical oceanography, 131(612), 2961-3012.

Zuo, H., Balmaseda, M. A., Tietsche, S., Mogensen, K., and Mayer, M.: The ECMWF operational ensemble reanalysis–analysis system for ocean and sea ice: a description of the system and assessment, Ocean Sci., 15, 779–808, https://doi.org/10.5194/os-15-779-2019, 2019